Biomedical Materials

SPECIAL ISSUE PAPER

# *In vitro* elastogenesis: instructing human vascular smooth muscle cells to generate an elastic fiber-containing extracellular matrix scaffold

Svenja Hinderer[1,2], Nian Shen[1,2], Léa-Jeanne Ringuette[3], Jan Hansmann[4], Dieter P Reinhardt[5], Sara Y Brucker[2], Elaine C Davis[3] and Katja Schenke-Layland[1,2,6]

[1] Department of Cell and Tissue Engineering, Fraunhofer Institute for Interfacial Engineering and Biotechnology (IGB), 70569 Stuttgart, Germany
[2] Department of Women's Health, Research Institute for Women's Health, Eberhard Karls University Tübingen, 72076 Tübingen, Germany
[3] Department of Anatomy and Cell Biology, McGill University, Montreal, Quebec H3A 0C7, Canada
[4] Institute for Tissue Engineering and Regenerative Medicine, University of Würzburg, 97070 Würzburg, Germany
[5] Department of Anatomy and Cell Biology and Faculty of Dentistry, McGill University, Montreal, Quebec H3A 0C7, Canada
[6] Department of Medicine/Cardiology, Cardiovascular Research Laboratories, David Geffen School of Medicine at UCLA, Los Angeles, CA, USA

**E-mail:** katja.schenke-layland@igb.fraunhofer.de

**Keywords:** elastin, elastic fibers, electrospinning, tissue engineering, regenerative medicine, heart valve, cardiovascular

OPEN ACCESS

RECEIVED
26 October 2014

REVISED
13 February 2015

ACCEPTED FOR PUBLICATION
15 February 2015

PUBLISHED
18 March 2015



## Abstract

Elastic fibers are essential for the proper function of organs including cardiovascular tissues such as heart valves and blood vessels. Although (tropo)elastin production in a tissue-engineered construct has previously been described, the assembly to functional elastic fibers *in vitro* using human cells has been highly challenging. In the present study, we seeded primary isolated human vascular smooth muscle cells (VSMCs) onto 3D electrospun scaffolds and exposed them to defined laminar shear stress using a customized bioreactor system. Increased elastin expression followed by elastin deposition onto the electrospun scaffolds, as well as on newly formed fibers, was observed after six days. Most interestingly, we identified the successful deposition of elastogenesis-associated proteins, including fibrillin-1 and -2, fibulin-4 and -5, fibronectin, elastin microfibril interface located protein 1 (EMILIN-1) and lysyl oxidase (LOX) within our engineered constructs. Ultrastructural analyses revealed a developing extracellular matrix (ECM) similar to native human fetal tissue, which is composed of collagens, microfibrils and elastin. To conclude, the combination of a novel dynamic flow bioreactor and an electrospun hybrid polymer scaffold allowed the production and assembly of an elastic fiber-containing ECM.

S Online supplementary data available from stacks.iop.org/BMM/10/034102

## 1. Introduction

The extracellular matrix (ECM) is a complex assembly of structural and functional proteins that are maintained by the resident cells. The cells not only secrete and assemble the ECM, but also respond to cues from the matrix that can alter cell behavior and maintain homeostasis. Elastic fibers within the ECM are crucial for tissue resilience and elasticity [1–3]. They play a major role during normal organ development [4] and are important structural components ensuring the proper function of adult tissues such as heart valves and blood vessels [5, 6]. During development, the soluble precursor named tropoelastin is aggregated on the cell surface and finally forms the mature elastic fiber in the extracellular space, assisted by proteins such as fibrillins, fibulins, fibronectin, lysyl oxidase and many more (figure 1) [3, 7]; however, the exact process of elastic fiber assembly remains poorly understood.

Inducing elastogenesis in a tissue-engineered construct would not only enable the production of functional implants but also the generation of advanced human-based *in vitro* test systems. These elastic fiber-containing systems could either be used to further understand the process of elastic fiber assembly or to study processes that are attributed to elastic fiber

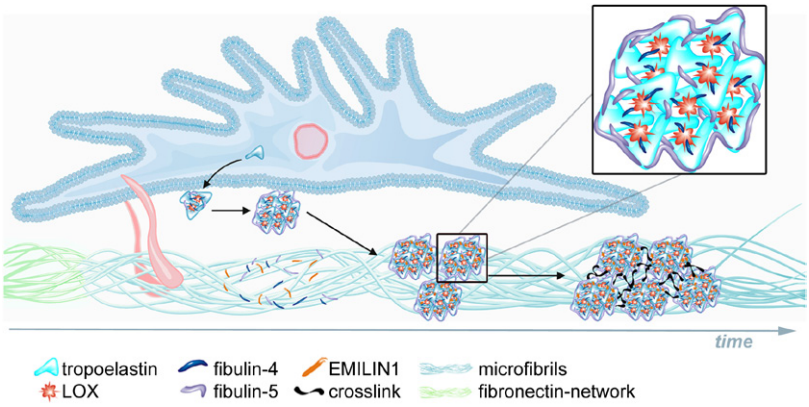


**Figure 1.** Principle of elastogenesis. Soluble tropoelastin is secreted by the cell and agglomerates on the cell surface. Simultaneously, microfibrils assemble in the extracellular space in the same location where fibronectin preexists. The fibrillin-1 and fibrillin-2 containing microfibrils are linked to a cell integrin (pink). The tropoelastin/elastin aggregates are then transferred to the microfibrils, where they further coalesce and form the mature elastic fiber via LOX crosslinking (modified from [3, 7]).

degeneration, including ageing. However, the *in vitro* generation of elastic fibers represents a major bottleneck in tissue engineering. Neonatal or adult rat vascular smooth muscle cells (VSMCs) and neonatal human dermal fibroblasts are routinely used to synthesize tropoelastin *in vitro*, and although elastin deposition can be shown in two-dimensional (2D) cell cultures [1, 8, 9], there have been no reports of the generation of functional human-based elastic fibers in three-dimensional (3D) tissue-engineered constructs [10–12]. Although it has been previously described that biochemical and biophysical factors impact elastin gene and protein expression in 3D tissue-engineered constructs, elastic fiber assembly in the extracellular space has not been shown [13].

Bioreactor systems have been designed to mimic the physiological and tissue-specific *in vivo* environment [14–17]. Such systems can potentially assist in the induction of elastogenesis in controlled *in vitro* experimental settings. To mimic the cellular environment and thus guide cell proliferation and migration, 3D substrates have also been used [5, 18, 19]. Electrospinning is one method used to generate 3D substrates and has been studied intensively for tissue engineering applications. With electrospinning, it is possible to generate scaffolds that provide not only three-dimensionality, but also mimic the natural ECM architecture [20–23].

We hypothesize that an optimal engineered microenvironment providing three-dimensionality and defined biochemical features, combined with biophysical signals can instruct cells to produce their own functional elastic fiber-containing ECM. Therefore, we designed a bioreactor and 3D electrospun hybrid scaffolds to expose primary-isolated human VSMCs to defined shear stress and topographies. Comprehensive ultrastructural and immunohistological studies were performed to verify the presence of an elastic fiber-containing network, including elastogenesis-associated proteins.

## 2. Materials and methods

### 2.1. 3D scaffold fabrication

Electrospun scaffolds were generated by dissolving equal amounts of poly (ethylene glycol) dimethacrylate (PEGdma; $M_n$ 2,000, 687529, Sigma, Steinheim, Germany) and poly (L-lactide) (PLA; $M_n$ 59,000, 93578, Sigma) with 1% photoinitiator (2-hydroxy-4′-(2-hydroxyethoxy)-2-methylpropiophenone; 410896, Sigma) in 1,1,1,3,3,3-hexafluoro-2-propanol (804515, Merck, Darmstadt, Germany). The polymer solution was processed into a 200 $\mu$m thick fiber mat employing a customized electrospinning device, 20 G nozzle, flat collector, and an electrode distance of 18 cm and 18 kV as described before [22]. Scaffolds were cross-linked with UV (365 nm) and sterilized using 70% ethanol prior to cell seeding. Detailed information about electrospinning parameter and mechanical scaffold properties can be obtained from Hinderer *et al* [22].

### 2.2. Cell culture experimental design and substrate treatment

Carotid arteries and saphenous veins were obtained from patients undergoing bypass surgery ($n = 3$; 50–65 years) (IRB #694/2012BO1 and F-2011–068). VSMCs were isolated as previously described [24].

2D experiments were performed using six-well culture inserts for dynamic culture and twelve-well culture inserts for the static control (Greiner Bio-One, Frickenhausen, Germany). Electrospun PEGdma-PLA scaffolds were used for 3D experiments. 2D membranes and 3D scaffolds were used either uncoated, or they were coated with a 1:5 mixture of 1% hyaluronic acid (HA; Advanced BioMatrix Inc., San Diego, USA) in PBS prior cell seeding, since HA had been reported to assists in tropoelastin crosslinking. For six- and twelve-well membranes, as well as electrospun scaffolds, we used $2 \times 10^4$, $9 \times 10^4$ or $3 \times 10^5$ cells per substrate. Twenty four hours after cell seeding, the substrates were transferred to the bioreactor. Depending on the experiment,

3.2 ng ml$^{-1}$ transforming growth factor beta 1 (TGF$\beta$1; Sigma-Aldrich) was added to the VSMC medium (C-22062, Promocell, Heidelberg, Germany).

### 2.3. Bioreactor system

The bioreactor was designed using SolidWorks for computer-aided design (Solidworks2010, Dassault Systèmes SolidWorks Corporation, Ludwigsburg, Germany). Furthermore, we developed a computational model to characterize the hydrodynamics of the designed bioreactor. Both, shear stress and laminar flow physics (Reynolds number) were calculated by a numerical approximated solution of the Navier–Stokes-Equation. Implementation, meshing and calculation were performed in Comsol 4.0 (COMSOL Multiphysics GmbH, Berlin, Germany). The simulations were carried out using bioreactor geometry and dimension. Moreover, a generalized minimal residual method (GMRES) was applied as the solver. The initial value for temperature was set to 37 °C. Based on the simulations, pump settings were defined in order to generate specific shear stress conditions.

For the *in vitro* experiments, the one-chamber perfusion bioreactor was connected to a closed tubing system (SC0746; Ismatec, Wertheim-Mondfeld, Germany) containing a 30 ml medium reservoir. The medium was pumped from the reservoir through the system using a peristaltic pump with a CA8 pump head and cassette (Ismatec, Glattbrugg, Switzerland). Briefly, the medium entered the bioreactor system through the inlet port, transited the flow chamber (1.5 × 1 × 0.7 cm) where the cell-seeded substrate was clamped in, and left the reactor through the outlet port. Furthermore, a filter (6901-2502; Whatman GmbH, Dassel, Germany) allowed permanent gas exchange, while the medium was pumped through the system. In order to carefully adapt the cells to the flow without shearing them off, the flow rate was initially set at 0.74 ml min$^{-1}$ and then adjusted to 1.48 ml min$^{-1}$ on the second day. After applying constant shear stress, the substrates were harvested and analyzed.

### 2.4. Immunofluorescence staining and imaging

Samples were processed for immunostaining employing previously described methods [4]. Polyclonal rabbit IgG anti-elastin (1:200; ab23747, Abcam, Cambridge, UK), anti-elastin microfibril interface located protein 1 (EMILIN-1; 1:500; HPA002822, Sigma-Aldrich), anti-lysyl oxidase (LOX; 1:100; NB100-2527, Cambridge, UK), anti-fibronectin (1:500; A0245, Dako, Eching, Germany), anti-smooth muscle myosin heavy chain 11 (SM-myosin; 1:50; ab53219, Abcam), anti-calponin 1 (CNN1; 1:100; HPA014263, Sigma-Aldrich) and mouse IgG2a anti-alpha smooth muscle actin (αSMA; 1:250; A2547, Sigma-Aldrich) served as primary antibodies. Polyclonal rabbit IgG anti-fibrillin-1 and -2 (each 1:1000) and anti-fibulin-4 and -5 (each 1:500) were produced as previously described [25, 26]. Alexa Fluor 488- and 594-conjugated goat anti-rabbit IgG (H+L) were applied as secondary antibodies (1:250; Life Technologies GmbH, Molecular Probes, Darmstadt, Germany). 4′,6-Diamidin-2-phenylindol (DAPI) was used to visualize cell nuclei and F-actin was observed with Alexa Fluor 594-conjugated phalloidin (1:100; A12381, Life Technologies GmbH). Images were taken with a LSM710 inverted confocal microscope (Carl Zeiss GmbH, Jena, Germany). For semi-quantification of elastin production, we used identical exposure times and laser intensities, and compared gray value intensities (GVI) of antibody-stained samples as previously described [4]. For each sample group, we used three specimens ($n = 3$).

### 2.5. RNA isolation and quantitative PCR analysis

Total RNA was extracted utilizing TRIzol (T9424, Sigmal-Aldrich) [27]. RNA with a RNA quality indicator (RQI) ≥ 8 was chosen for quantitative real-time polymerase chain reaction (qPCR). cDNA synthesis was performed using a Transcriptor First Strand cDNA-Synthesis Kit (04896866001, Hoffmann-La Roche AG, Basel, Switzerland) according to the manufacturer's instructions. qPCR was performed in 25 $\mu$l reaction volumes using a Chromo4 Real-time Thermal Cycler (Bio-Rad, Munich, Germany). qPCR amplicons were detected by fluorescence detection of SYBR Green (204054, QuantiFast SYBR Green PCR Kit, Qiagen). Cycling parameters were as follows: 95 °C for 5 min followed by 40 cycles at 95 °C for 10 s and 60 °C for 30 s. For gene expression profiling of elastin (ELN), fibulin-5 (FBLN5), fibrillin-1 (FBN1), fibronectin (FN1) and glyceraldehyde 3-phosphate dehydrogenase (GAPDH), we employed primers from Qiagen (human QuantiTect Primer Assay, Qiagen, Hilden, Germany).

### 2.6. Specific elastin autofluorescence detection

3D scaffolds and human elastin (SH476, EPC, Owensville, USA) were rinsed with DPBS and transferred to glass-bottom dishes. The Mai Tai laser of a LSM710 (Carl Zeiss GmbH) was used to excite the samples with a wavelength of 760 nm [28, 29]. Emissions between 440 and 500 nm were detected and analyzed utilizing Zeiss software (Carl Zeiss GmbH).

### 2.7. Scanning and transmission electron microscopy

A scanning electron microscope (1530 VP Zeiss, Carl Zeiss GmbH) was used to visualize the fibers of the electrospun scaffolds, which were mounted onto stubs and sputtered with platinum. Cell-seeded scaffolds were fixed with 2% glutaraldehyde, dehydrated with ethanol and dried at room temperature before mounting and sputtering. Transmission electron microscopy (TEM) was performed as described before [30] on electrospun scaffolds, 6 d dynamically cultured electrospun scaffolds and 18 week human valves (UCLA IRB #05-10-093). Briefly, all samples were fixed with 3% glutaraldehyde in 0.1 M sodium cacodylate buffer (pH 7.4). The samples were treated sequentially with

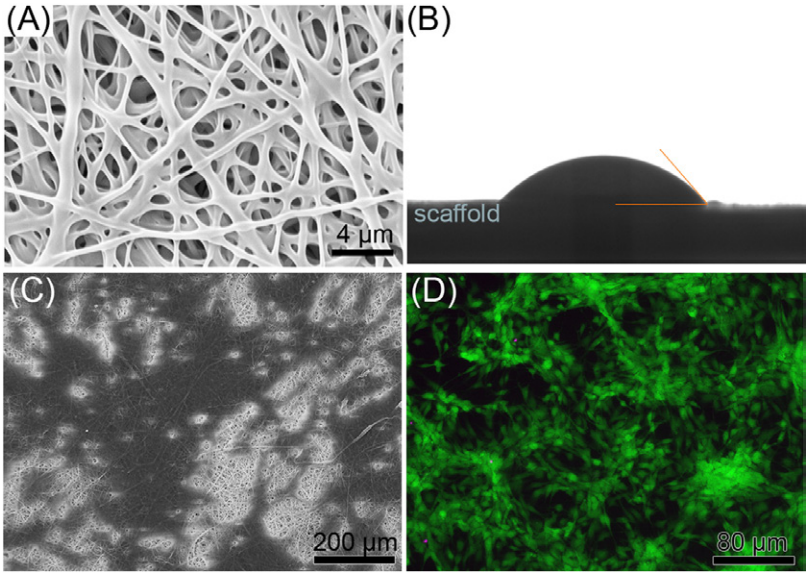


**Figure 2.** Scaffold characterization and cytotoxicity testing according to DIN EN ISO 10993. (*a*) Scanning electron micrograph of a hydrophilic UV-cross-linked electrospun PEGdma-PLA scaffold. (*b*) Water drop on the electropsun scaffold to determine wettability. A contact angle (orange) <90° indicates hydrophilicity. (*c*) SEM image of spread hFs seeded on the scaffold. (*d*) Live-dead staining of hFs after scaffold-extract contact. Living cells are green, dead cells are shown in red.

1% osmium tetroxide and 2% tannic acid, both in buffer and 2% uranyl acetate in water. After dehydration with a graded series of methanol to propylene oxide, the scaffolds and valves were infiltrated and embedded in Epon and polymerized for 3 d at 60 °C. The blocks were then sectioned (60 nm) and counterstained with methanolic uranyl acetate and lead citrate. For imaging, a FEI Tecnai 12 transmission electron microscope was used at 120 kV.

### 2.8. Live-dead staining

Primary human dermal fibroblasts (hFs) from adult skin were used in order to determine a potential cytotoxic effect of the electrospun scaffolds. This system is certified and accredited according to DIN EN ISO 10993–5. hFs were isolated using collagen digestion and seeded into chamber slides (Sigma-Aldrich). In parallel, extracts of soluble polymer compounds were prepared by incubating the electrospun scaffolds in Dulbecco's Modified Eagle Medium (DMEM; 11965-092, Life Technologies GmbH). After 48 h, the scaffolds were removed and the seeded hFs were incubated for another 48 h with the generated extracts. Fluorescein diacetate (FDA; F7378, Sigma Aldrich) and propidium iodide (PI; P4170, Sigma Aldrich) enabled the discrimination between living (green) and dead (red) cells in order to determine cytotoxic material effects. Stock solutions of 5 µg ml$^{-1}$ FDA in acetone and 0.5 µg ml$^{-1}$ PI in DPBS were prepared and stored at -20 °C. For live-dead staining, extracts were removed and a solution of 105 µL FDA, 95 µL PI and 3150 µL DMEM (serum free) was added. After 15 min incubation at 37 °C, the staining solution was replaced by DPBS for washing. Subsequently, images were taken with an Axio Observer fluorescence microscope (Carl Zeiss GmbH).

### 2.9. Contact angle measurement

Wettability was determined by deposing a 2 µl drop of $dH_2O$ onto the scaffolds as previously described [22]. Measurements were recorded using a DSA25S (Krüss, Hamburg, Germany).

### 2.10. Statistical analyses

One-way analysis of variance (ANOVA) was carried out to compare data groups. A probability value of 95% ($p < 0.05$) was used to determine significance. All data are presented as mean ± standard deviation.

## 3. Results

### 3.1. Scaffold and bioreactor design and evaluation

To create the 3D fibrous hybrid scaffolds, we electrospun PEGdma and PLA (figure 2(*a*) [22],). After UV-crosslinking of the dimethacrylate groups, a hydrophilic and non-cytotoxic scaffold with an average fiber diameter of 0.37 ± 0.08 µm was obtained (figures 2(*a*)–(*d*), [22]). A fluid-flow bioreactor was designed and fabricated to allow cultures of cell-seeded 2D membranes and 3D scaffolds to be exposed to defined fluid shear stress. A computer-aided design of the flow bioreactor showing the flow direction and the scaffold position is displayed in figures 3(*a*) and (*b*). To determine optimal fluid mechanics, simulations were performed (figures 3(*c*) and (*d*)) and a Reynolds number of approximately 1 was identified. The red stream lines in figure 3(*c*) indicate that no turbulences occurred, and a Reynolds number <2300 confirmed laminar flow conditions in the bioreactor. With a flow rate of 1.48 ml min$^{-1}$, a constant shear stress between 6 × 10$^{-4}$ and 11 × 10$^{-4}$ dyne cm$^{-2}$ (equal to 6–11 × 10$^{-5}$ Pa) was applied over the entire scaffold.

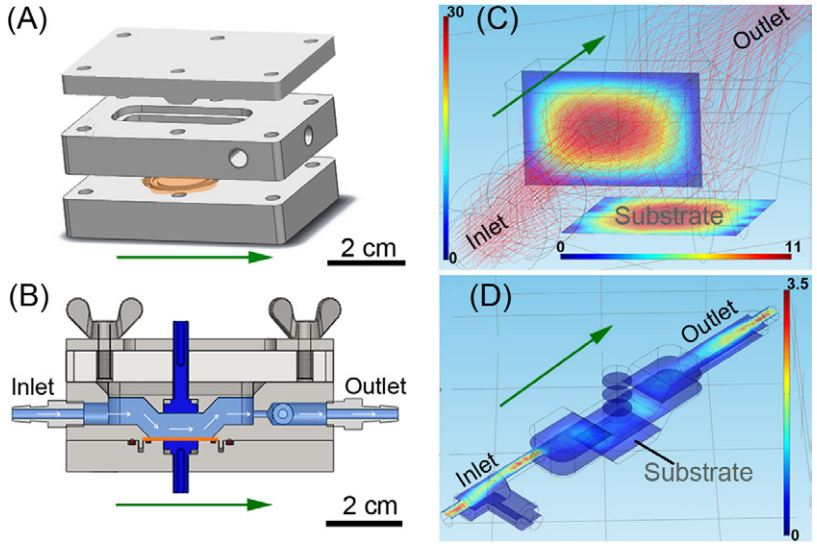


**Figure 3.** Design and simulation of the bioreactor system. Computer-aided design of (*a*) the single bioreactor components and (*b*) the flow bioreactor in a cross-sectional view. The cell-seeded substrate is highlighted in orange. (*c*, *d*) Simulations displayed in top view: (*c*) simulation of wall shear stress distribution in the bioreactor system ($\times 10^{-4}$ dyne cm$^{-2}$); red streamlines and (*d*) a Reynolds number of <2300 indicate laminar flow. Green arrows indicate the flow direction of the medium.

### 3.2. Influence of shear stress, three-dimensionality and biochemical aspects

For cell culture experiments, 2D and 3D, uncoated and HA-coated substrates were seeded with primary isolated, CNN1-, αSMA- and SM-myosin-expressing VSMCs and cultured for 3 or 6 d (figure 4). We observed cell alignment on the 2D membranes, perpendicular to the direction of flow, starting at 6 d of dynamic culture (figures S1(*a*)–(*h*) (stacks.iop.org/BMM/10/034102)). In general, under all culture conditions, the 6 d cultures revealed significantly higher ELN expression and protein production when compared to the 3 d cultures. Moreover, after 6 d, a significant shear stress-induced up-regulation of ELN and elastin protein was observed when comparing the dynamic bioreactor cultures to the static controls (elastin protein: 3.11 ± 0.34 (dynamic) versus 2.4 ± 0.21 (static), $p = 0.026$; ELN: 8.49 ± 2.68 (dynamic) versus 4.43 ± 0.11 (static), $p = 0.0065$; figures S1(*i*) and (*j*) (stacks.iop.org/BMM/10/034102)). No significant differences were detected between uncoated controls and HA-coated samples in either static or dynamic cultures (figure S1). Since TGF$\beta$1 participates in matrix regulation [8], we added TGF$\beta$1 [31] to the dynamic 2D and 3D cultures. After 6 d, the substrates were stained for elastin and quantified (figure 5 and figure S2 (stacks.iop.org/BMM/10/034102)). Significantly higher elastin production was detected in TGF$\beta$1-treated 2D cultures compared to cultures without TGF$\beta$1 (figure S2(*a*)); however, no significant difference was observed for ELN expression in these samples (figure S2(*b*)). Semi-quantification of the immunofluorescence images revealed a significant increase in elastin production on the 3D hybrid scaffolds compared to the 2D membranes (figure S2(*c*)); 7.33 ± 0.58 3D versus 4.15 ± 0.67 2D, $p = 0.003$). This increase was not seen at the gene level (figure S2(*d*)).

### 3.3. Induction of elastogenesis and ECM development on 3D scaffolds

Interestingly, we observed deposition of elastin on the hydrophilic electrospun fibers, and elastin-positive fibers were detected in between cells (figures 5(a) and (*b*)). TEM further revealed the presence of long bundles of 'coated' microfibrils in between the cells (figures 5(*c*) and (*d*)). Indeed, electron-dense material could often be identified within these bundles (figure 5(*d*)). Moreover, analyzing the cell-seeded fibrous electrospun matrix using multiphoton laser-induced autofluorescence imaging as previously described [29], emission patterns comparable to those of pure human elastin were detected (figures 5(*e*)–(*j*)). In contrast, this specific elastin autofluorescence and the corresponding emission patterns did not occur on the scaffold cultured under the same conditions without cells (figures 5(*g*) and (*j*)).

Elastic fiber formation depends not only on sufficient tropoelastin synthesis, but also on proper matrix assembly and crosslinking. We therefore performed immunofluorescence staining to determine the presence of important elastogenesis-associated proteins in our cultures and identified that after a 6 d dynamic culture of VSMCs on the 3D HA-coated scaffold, fibrillin-1 and -2, fibronectin, fibulin-4 and -5 and EMILIN-1 (figures 6(*a*)–(*f*)), as well as the cross-linking enzyme LOX (figure S3 (stacks.iop.org/BMM/10/034102)) were all produced. Although TGF$\beta$1 and three-dimensionality had no significant impact on ELN expression, a significant increase of FBLN5 and FBN1 expression was observed by adding TGF$\beta$1 (figures S2(*e*) and (*f*)). FBN1 and FN1

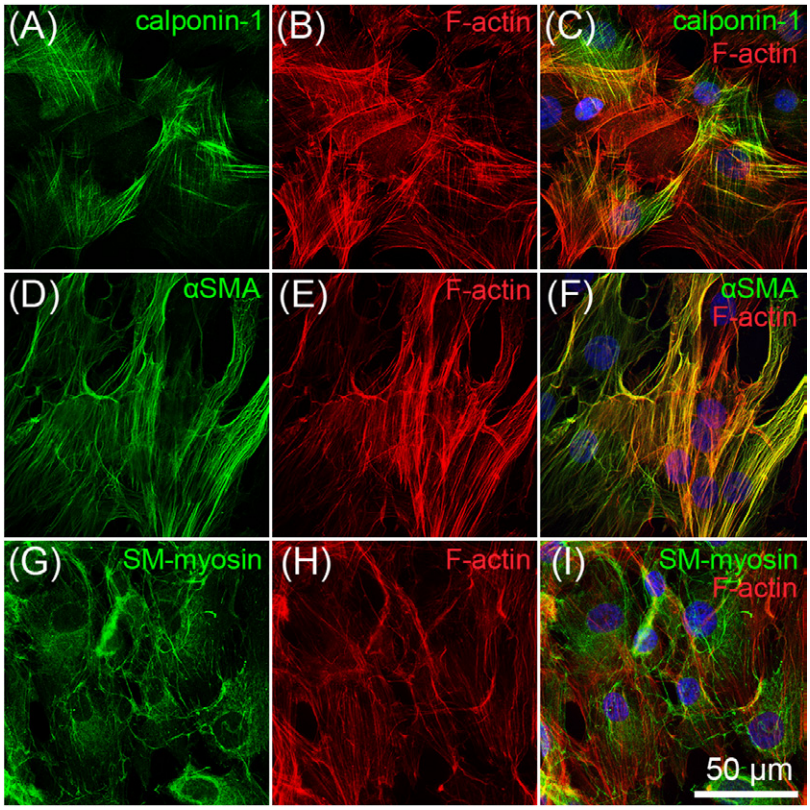


**Figure 4.** VSMC characterization. Immunofluorescence staining of calponin-1, αSMA and SM-myosin (all green) expressing VSMCs. F-actin is shown in red and the cell nuclei are visualized with DAPI (blue).

levels were significantly up-regulated in 3D cultures when compared to 2D controls (figures S2(*f*) and (*g*)). Moreover, TEM analyses revealed a proper and well-developed ECM in the tissue-engineered constructs, including the presence of collagens, microfibrils and elastin, similar to the native fetal heart valve ECM (figures 6(*g*)–(*i*)).

## 4. Discussion

It was previously demonstrated that mimicking physiological conditions such as shear stress [14] or three-dimensionality [32] supports tissue maturation. Therefore, we designed a fluid flow bioreactor system, which is suitable for the culture of 3D cell-seeded tissue-engineered scaffolds. The defined and applied shear stress in this study differs from physiological blood luminal flow, but instead corresponds to the *in vivo* situation, where VSMCs are exposed to a very low transmural interstitial flow rather than direct shear stress [33]. VSMC alignment was observed after 6 d of culture, a phenomenon that has been previously described when VSMCs are exposed to laminar shear stress [33]. Furthermore, a shear stress-induced up-regulation of tropoelastin/elastin synthesis was observed comparing the dynamic cultures to the static controls. There was no significant impact on elastin expression due to HA coating of the substrates. The HA used in this study has a molecular weight of ~750 000 Da. Although high molecular weight HA (>10 000 Da) does not induce elastin precursor synthesis, this type of HA supports elastic matrix deposition and more efficient crosslinking [34]. Smaller HA molecules do enhance elastin precursor synthesis [35]; however, due to its proposed capacity to support tropoelastin crosslinking, the larger HA was used in our experiments. The addition of TGF$\beta$1 increased elastin protein synthesis as well as FBLN5 and FBN1 expression, but did not enhance ELN expression. The obtained results indicate that TGF$\beta$1 has no direct impact on ELN expression, but may be crucial for protein binding and elastic fiber assembly since TGF$\beta$1 stabilizes elastin mRNA and facilitates tropoelastin recruitment for elastic fiber assembly [8, 36, 37].

In addition, we observed a positive effect on elastin protein expression as well as elastin deposition and new fiber formation on the 3D scaffolds. Lin *et al* described in their 4 d-study a direct impact of three-dimensionality on ELN gene expression [31], which is in contrast to our experimental data based on which we did not identify such an effect of three-dimensionality on the ELN gene expression. We assume that these discrepancies are either due to the different culture periods or caused by the application of another type of material [31]. An explanation for the increased elastin protein level on 3D scaffolds is that the fibrous electrospun matrix has a higher surface area and therefore more proteins, growth factors and other signaling

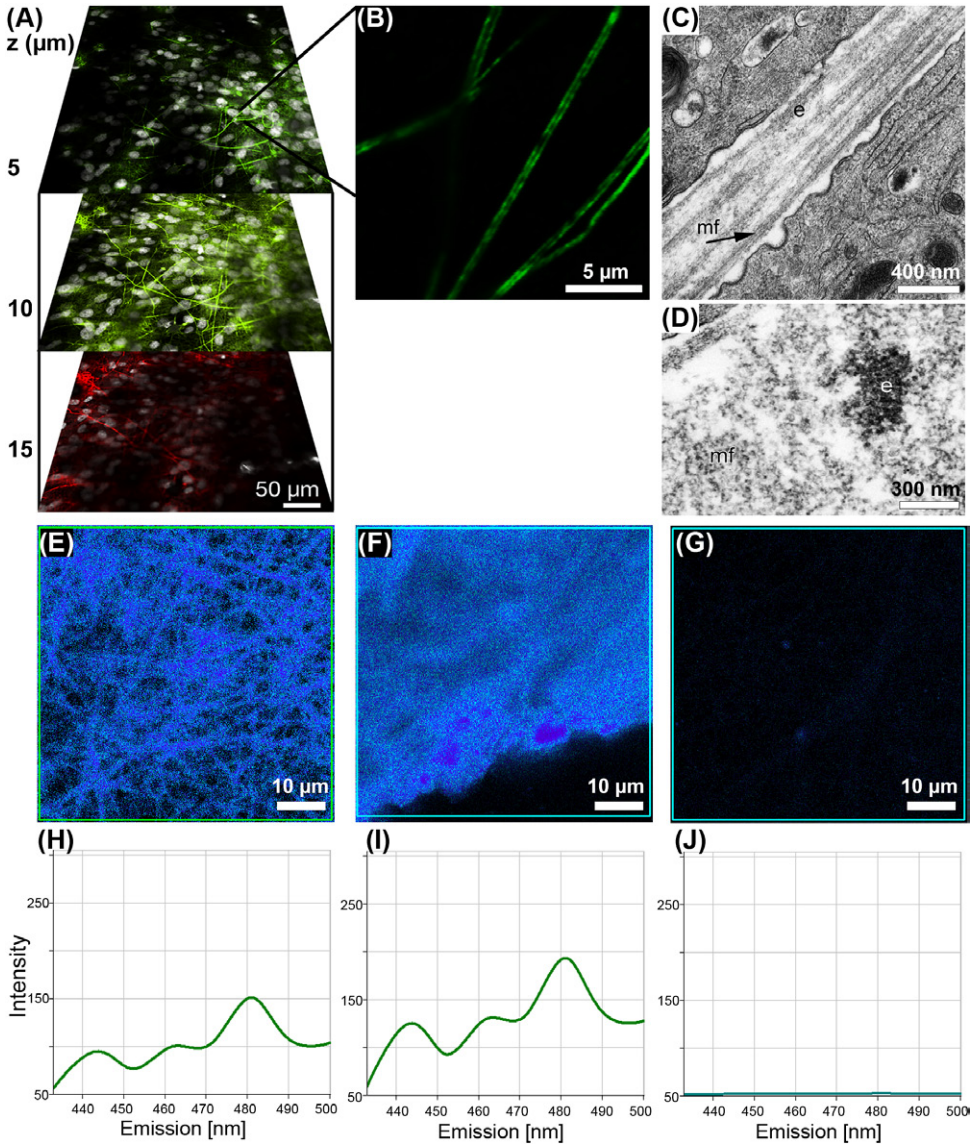


**Figure 5.** Elastin protein expression and deposition. ECM characterization of 3D HA-coated scaffolds after 6 d of dynamic culture with presence of TGF$\beta$1. (*a*) Optical sections of the immunohistologically stained samples show elastin in green (5 $\mu$m), yellow (10 $\mu$m) and red (15 $\mu$m). Cell nuclei are white. (*b*) High-magnified optical section of an elastin-stained fiber (green). (*c*, *d*) TEM images of a tissue-engineered construct after 6 days of dynamic culture. (*c*) Long bundles of coated microfibrils (mf; black arrow) and developing elastic fibers (*e*) between two VSMCs. (*d*) Microfibrils (mf) and electron-dense elastin (*e*, black) seen in cross-section in the newly formed ECM. (*e*)–(*j*) Multiphoton laser-induced elastin autofluorescence detection at 760 nm. (*e*) Cell-seeded scaffold after bioreactor culture, (*f*) human elastin, (*g*) the un-seeded, pure scaffold and (*h*)–(*i*) the corresponding emission spectra.

molecules can attach [5, 20]. Based on these results we conclude that the HA-coated electrospun PEGdma-PLA scaffold allows bio-functionalization with elastin *in vitro*. More interestingly, immunohistological analyses revealed newly formed elastin-containing fibers in between the layers of VSMCs. Ultrastructural assessment of the newly assembled ECM confirmed the presence of long bundles of coated microfibrils. It has previously been described that both smooth and 'naked' microfibrils as well as microfibrils coated with accessory proteins such as tropoelastin and fibronectin exist in the ECM [38, 39]. In our study, the microfibrils coated with protein could represent developing/maturing elastic fibers.

Tropoelastin is the soluble ~70 kDa elastin precursor. Tropoelastin monomers coacervate under physiological conditions and are cross-linked in the presence of fibrillin-containing microfibrils to form insoluble elastic fibers [3, 4, 7, 40]. The initial self-assembly of elastin and the significance of fibrillins and fibulins has been extensively studied [9, 41, 42], and the complex interactions between elastogenesis-associated proteins have been comprehensively reviewed [7, 43]. Accordingly, the successful assembly of elastic fibers is highly dependent on the elastogenesis-associated proteins, which were all present in our study after 6 d of *in vitro* culture. In addition, transmission electron micrographs revealed a newly formed ECM comparable to the one seen in 18 week fetal heart tissues. Although the elastin detected in the tissue-engineered constructs was not as dense as seen in the native 18 week matrix, it must be considered that the observation was made after only 6 d *in vitro*. Our

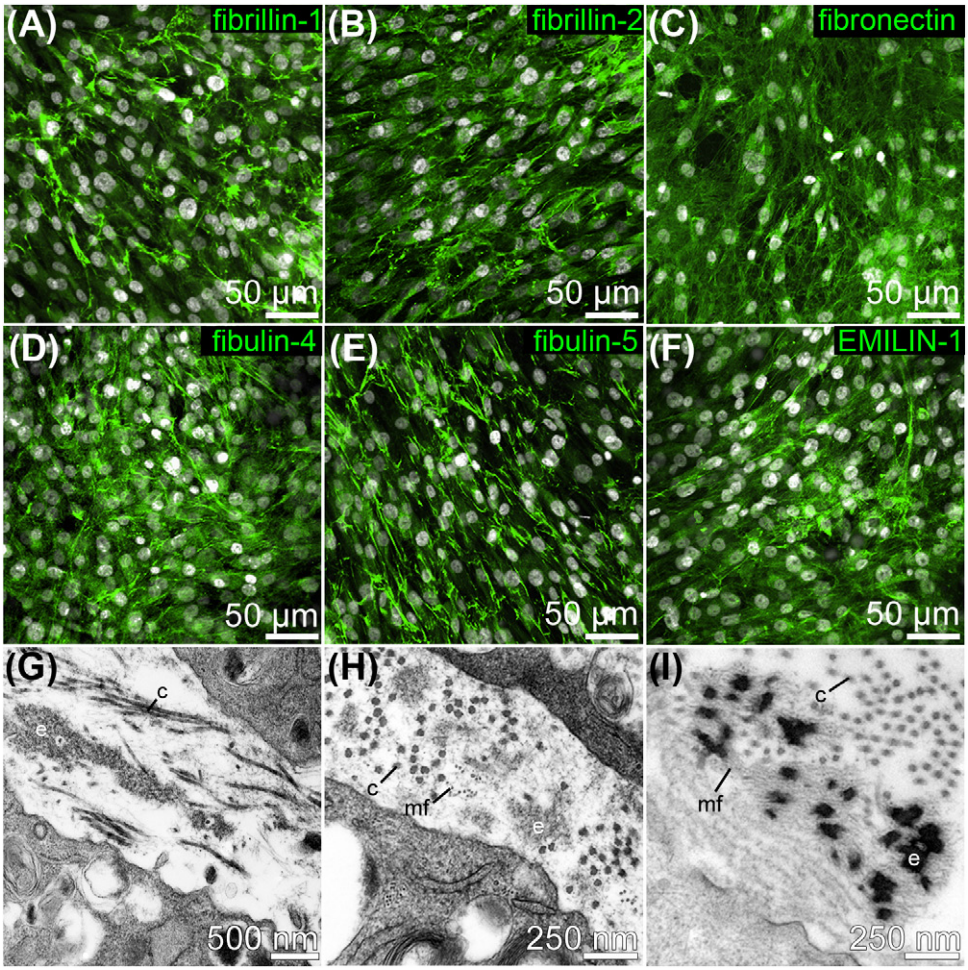


**Figure 6.** ECM assembly within the tissue-engineered construct. (*a*)–(*f*) Immunofluorescence staining of elastogenesis-associated proteins after a 6 d dynamic culture on 3D HA-coated scaffolds with TGF$\beta$1. (*g*, *h*) TEM images of the 3D cultured construct show a developing ECM comparable to (*i*) a 18 week human fetal heart valve collagen (*c*), microfibrils (*mf*), elastin (*e*)

results display therefore a developing but not yet completely matured elastic fiber-containing ECM.

## 5. Conclusion

We conclude that the customized bioreactor described in this study, combined with a hybrid fibrous 3D polymer scaffold, is a promising tool to induce ECM formation, including the production of elastin and elastic fiber-related proteins, which are necessary for the assembly of mature elastic fibers. To our knowledge, this is the first report of the 3D *in vitro* generation of elastic fibers, which addresses a major bottleneck in the fields of tissue engineering and regenerative medicine. This technology can be utilized not only for *in vitro* elastogenesis studies, but moreover, our system can potentially serve as a platform technology to engineer elastic fiber-rich tissues and organs such as heart valves and blood vessels. In our study, we employed a biocompatible poly (ethylene glycol)-based scaffold that can be potentially bio-functionalized with human elastin and instruct cells to develop their own ECM. This is highly advantageous when aiming for applications in regenerative medicine and medical device development.

## 6. Limitations and future work

In this study, the described bioreactor system enabled the induction of elastogenesis on an electrospun PEG-dma-PLA scaffold. The size of the flow chamber is sufficient when aiming for an introduction of elastic fibers within a 2D or 3D cell culture test system; however, the systematic up-scaling of this system will be required in order to generate clinically relevant tissues. Furthermore, in this study we used primary isolated human VSMCs. A limiting factor with these cells is that they are isolated from veins and arteries, which is unfavorable when producing patient-tailored implants due to the limited number and variation in quality. Therefore, the identification of alternative cell sources, for example by utilizing autologous adult stem cell-derived or induced-pluripotent stem cell-derived cardiovascular progenitor cells or VSMC, will be necessary.

## Acknowledgments

The authors thank A Kahlig (IGVP, University Stuttgart), S Geist and A-L Tremmer (both Dept. of Women's Health, Eberhard Karls University

Tübingen) for their technical support, and S L Layland (Fraunhofer IGB Stuttgart) for his helpful comments on the manuscript. The authors are grateful for financial support from the Fraunhofer-Gesellschaft Internal programs (Attract 692263 to KSL), the Ministry of Science, Research and the Arts of Baden-Württemberg (33-729.55-3/214 and SI-BW 01222-91 to KSL), Canadian Institutes of Health Research (MOP-106494 to DPR) and the Natural Sciences and Engineering Research Council of Canada (355710 to ECD; 375738-09 to DPR).

## References

[1] Hirai M, Horiguchi M, Ohbayashi T, Kita T, Chien K R and Nakamura T 2007 Latent TGF-$\beta$-binding protein 2 binds to DANCE/fibulin-5 and regulates elastic fiber assembly *EMBO J.* **26** 3283–95
[2] Nakamura T *et al* 2002 Fibulin-5/DANCE is essential for elastogenesis *in vivo Nature* **415** 171–5
[3] Kielty C M, Sherratt M J and Shuttleworth C A 2002 Elastic fibres *J. Cell Sci.* **115** 2817–28
[4] Votteler M *et al* 2013 Elastogenesis at the onset of human cardiac valve development *Development* **140** 2345–53
[5] Bashur C A, Venkataraman L and Ramamurthi A 2012 Tissue engineering and regenerative strategies to replicate biocomplexity of vascular elastic matrix assembly *Tissue Eng.* B **18** 203–17
[6] Waterhouse A, Wise S G, Ng M K and Weiss A S 2011 Elastin as a nonthrombogenic biomaterial *Tissue Eng.* B **17** 93–9
[7] Wagenseil J E and Mecham R P 2007 New insights into elastic fiber assembly *Birth Defects Res.* C *Embryo Today* **81** 229–40
[8] Kothapalli C R, Taylor P M, Smolenski R T, Yacoub M H and Ramamurthi A 2008 Transforming growth factor $\beta$ 1 and hyaluronan oligomers synergistically enhance elastin matrix regeneration by vascular smooth muscle cells *Tissue Eng.* A **15** 501–11
[9] Noda K *et al* 2013 Latent TGF-$\beta$ binding protein 4 promotes elastic fiber assembly by interacting with fibulin-5 *Proc. Natl Acad. Sci. USA* **110** 2852–7
[10] Opitz F *et al* 2004 Tissue engineering of aortic tissue: dire consequence of suboptimal elastic fiber synthesis *in vivo Cardiovasc. Res.* **63** 719–30
[11] Weber B *et al* 2013 Off-the-shelf human decellularized tissue-engineered heart valves in a non-human primate model *Biomaterials* **34** 7269–80
[12] L'Heureux N *et al* 2006 Human tissue-engineered blood vessels for adult arterial revascularization *Nat. Med.* **12** 361–5
[13] Venkataraman L, Bashur CA and Ramamurthi A 2014 Impact of cyclic stretch on induced elastogenesis within collagenous conduits *Tissue Eng.* A **20** 1403–15
[14] Pusch J *et al* 2011 The physiological performance of a 3D model that mimics the microenvironment of the small intestine *Biomaterials* **32** 7469–78
[15] Zorlutuna P *et al* 2012 Microfabricated biomaterials for engineering 3D tissues *Adv. Mater.* **24** 1782–804
[16] Tranquillo RT 2002 The tissue-engineered small-diameter artery *Ann. N. Y. Acad. Sci.* **961** 251–4
[17] Kim B S, Nikolovski J, Bonadio J and Mooney D J 1999 Cyclic mechanical strain regulates the development of engineered smooth muscle tissue *Nat. Biotechnol.* **17** 979–83
[18] Rnjak-Kovacina J *et al* 2011 Tailoring the porosity and pore size of electrospun synthetic human elastin scaffolds for dermal tissue engineering *Biomaterials* **32** 6729–36
[19] Hahn M S, Miller J S and West J L 2006 3D biochemical and biomechanical patterning of hydrogels for guiding cell behavior *Adv. Mater.* **18** 2679–84
[20] Agarwal S, Wendorff J H and Greiner A 2009 Progress in the field of electrospinning for tissue engineering applications *Adv. Mater.* **21** 3343–51
[21] Schenke-Layland K *et al* 2011 Recapitulation of the embryonic cardiovascular progenitor cell niche *Biomaterials* **32** 2748–56
[22] Hinderer S *et al* 2014 Engineering of a bio-functionalized hybrid off-the-shelf heart valve *Biomaterials* **35** 2130–9
[23] Kim T G, Shin H and Lim D W 2012 Biomimetic scaffolds for tissue engineering *Adv. Funct. Mater.* **22** 2446–68
[24] Opitz F, Schenke-Layland K, Cohnert T U and Stock U A 2007 Phenotypical plasticity of vascular smooth muscle cells-effect of *in vitro* and *in vivo* shear stress for tissue engineering of blood vessels *Tissue Eng.* **13** 2505–14
[25] Tiedemann K, Bätge B, Müller P K and Reinhardt D P 2001 Interactions of fibrillin-1 with heparin/heparan sulfate, implications for microfibrillar assembly *J. Biol. Chem.* **276** 36035–42
[26] El-Hallous E *et al* 2007 Fibrillin-1 interactions with fibulins depend on the first hybrid domain and provide an adaptor function to tropoelastin *J. Biol. Chem.* **282** 8935–46
[27] Schenke-Layland K, Angelis E, Rhodes K E, Heydarkhan-Hagvall S, Mikkola H K and Maclellan W R 2007 Collagen IV induces trophoectoderm differentiation of mouse embryonic stem cells *Stem Cells* **25** 1529–38
[28] Konig K, Schenke-Layland K, Riemann I and Stock U A 2005 Multiphoton autofluorescence imaging of intratissue elastic fibers *Biomaterials* **26** 495–500
[29] Schenke-Layland K *et al* 2009 Cardiomyopathy is associated with structural remodelling of heart valve extracellular matrix *Eur. Heart J.* **30** 2254–65
[30] Davis E C 1993 Smooth muscle cell to elastic lamina connections in developing mouse aorta. Role in aortic medial organization *Lab. Invest.* **68** 89–99
[31] Lin S, Sandig M and Mequanint K 2011 3D topography of synthetic scaffolds induces elastin synthesis by human coronary artery smooth muscle cells *Tissue Eng.* A **17** 1561–71
[32] Heydarkhan-Hagvall S *et al* 2008 3D electrospun ECM-based hybrid scaffolds for cardiovascular tissue engineering *Biomaterials* **29** 2907–14
[33] Shi Z-D and Tarbell J 2011 Fluid flow mechanotransduction in vascular smooth muscle cells and fibroblasts *Ann. Biomed. Eng.* **39** 1608–19
[34] Joddar B and Ramamurthi A 2006 Fragment size- and dose-specific effects of hyaluronan on matrix synthesis by vascular smooth muscle cells *Biomaterials* **27** 2994–3004
[35] Joddar B and Ramamurthi A 2006 Elastogenic effects of exogenous hyaluronan oligosaccharides on vascular smooth muscle cells *Biomaterials* **27** 5698–707
[36] Sommer N, Sattler M, Weise J M, Wenck H, Gallinat S and Fischer F 2013 A tissue-engineered human dermal construct utilizing fibroblasts and transforming growth factor $\beta$1 to promote elastogenesis *Biotechnol. J.* **8** 317–26
[37] Kucich U, Rosenbloom J C, Abrams W R, Bashir M M and Rosenbloom J 1997 Stabilization of elastin mRNA by TGF-$\beta$: initial characterization of signaling pathway *Am. J. Respir. Cell Mol. Biol.* **17** 10–6
[38] Robb B W, Wachi H, Schaub T, Mecham R P and Davis E C 1999 Characterization of an *in vitro* model of elastic fiber assembly *Mol. Biol. Cell* **10** 3595–605
[39] Davis E C 1994 Immunolocalization of microfibril and microfibril-associated proteins in the subendothelial matrix of the developing mouse aorta *J. Cell Sci.* **107** 727–36
[40] Kielty C M, Wess T J, Haston L, Ashworth J L, Sherratt M J and Shuttleworth C A 2002 Fibrillin-rich microfibrils: elastic biopolymers of the extracellular matrix *J. Muscle Res. Cell Motil.* **23** 581–96
[41] Cirulis J T *et al* 2008 Fibrillins, fibulins, and matrix-associated glycoprotein modulate the kinetics and morphology of *in vitro* self-assembly of a recombinant elastin-like polypeptide *Biochemistry* **47** 12601–13
[42] Yanagisawa H *et al* 2002 Fibulin-5 is an elastin-binding protein essential for elastic fibre development *in vivo Nature* **415** 168–71
[43] Baldwin A K, Simpson A, Steer R, Cain S A and Kielty C M 2013 Elastic fibres in health and disease *Expert Rev. Mol. Med.* **15:e8**